

The International Journal for the Tunnelling Industry

Tunnelling Journal

www.tunnellingjournal.com

TUNNELLING JOURNAL DEC 2020/JAN 2021



Mighty breakthrough for Europe's biggest boring machine

Page
08

Predicting our post Covid future

The third of three papers in which our experts address the impacts of the Covid-19 Pandemic on our industry.

Page
14

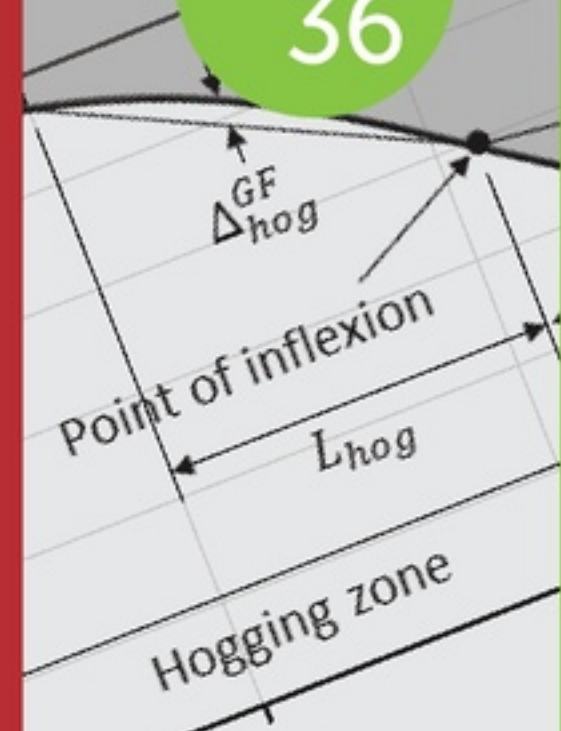
Happy new ideas!

We look forward to a better year and a host of new ideas and advances in 2021.

Page
36

Building damage assessment...

See part 1 of a fascinating report by Dr Benoît Jones and Dr Giorgia Giardina.



Contents

Editor's comment – page 5

News from the web – page 6

Predicting the Post Covid Future 3

08

This is the third and final paper in which Martin Knights, current Chair of London Bridge Associates (LBA) and Ex-President of the ITA and Bob Ibell Ex-Chair and Co-Founder of LBA and Ex-Chair of the BTS, consider the possible influences which could combine with the impacts of the Covid-19 Pandemic on our infrastructure and the tunnelling and construction industry.

Happy new idea!

14

As we look forward to a better year in 2021, we can also look forward to better projects, thanks to a host of new ideas and advances.

Santa Lucia XL EPBM crosses the finish line

24

In June 2020, Europe's largest TBM "Lucia" with a diameter of 15.87m, completed its mission to excavate the 7.5km long Santa Lucia highway tunnel, north of Florence, Italy. The machine and the project team mastered this extraordinary challenge in less than three years despite numerous challenges, the solutions to which were developed both beforehand and on-site.

The record breakers

31

The last few years have seen a flurry of new records being claimed on microtunnelling projects. Kristina Smith asks some industry experts what has caused this purple patch.

Building damage assessment using the simple beam method – Part 1

36

The maximum tensile strain is estimated by the 'simple beam method'. This method is outlined by Dr Benoît Jones, Managing Director, Inbye Engineering, and Dr Giorgia Giardina, Assistant Professor, Delft University of Technology in a fascinating report.

Contacts – page 42



Cover Story

HERRENKNECHT



Tunnelling Systems

June 2020, and celebrations at the Santa Lucia Tunnel in Northern Italy following the successful breakthrough of the project's Herrenknecht 15.87m diameter EPBM 'Lucia' - Europe's largest TBM. Close cooperation between Contractor Pavimental S.p.A, Client, Autostrade per l'Italia S.p.A, and Herrenknecht saw the mega-machine excavate the 7.5km long tunnel in under three years through a number of expected, and some less expected, challenging ground conditions.



Building damage assessment using the simple beam method – Part 1

Tunnelling invariably causes ground movements which have an impact on buildings along the tunnel route. Standard methods of estimating the potential damage to buildings have been in use since the 1970's. In the case of masonry load-bearing walls the level of damage may be estimated by predicting the maximum tensile strain and comparing it to limiting values established from case studies and full-scale testing of masonry walls. The maximum tensile strain is estimated by imposing the greenfield deflection ratio on the building modelled as a simple rectangular section beam with a centrally-applied point load, and this is known as the 'simple beam method'. This method is reviewed in this article and several corrections and clarifications are proposed. The corrections make a significant difference to the calculation of maximum strains in a building, which were underestimated in the standard approach.

By Dr Benoît Jones, Managing Director, Inbye Engineering, and Dr Giorgia Giardina, Assistant Professor, Delft University of Technology

It is necessary, and in many countries it is a legal or planning requirement, to assess buildings along the route of a tunnel for the risk of damage due to tunnelling settlements (e.g. for CTRL see Moss & Bowers, 2006, for Crossrail see Crossrail, 2008). This will usually follow a staged process. At each stage buildings are classified into one of six damage categories, from 0 to 5, as shown in Table 1, first proposed by Burland et al. (1977). Categories 0, 1 and 2 are aesthetic damage, 3 and 4 are serviceability damage, and 5 is the most severe category where stability of the building will be affected, and it may collapse. At the preliminary stage ('Stage 1'), very simple methods are used to conservatively assess the risk of settlement damage to all the buildings, with the aim that many of them can be ruled out as being at low risk. The remaining buildings will proceed to a second stage ('Stage 2'), where they will be analysed in more detail, again hoping that many more of them will be moved to the low risk category. Any remaining buildings will proceed to a third, more detailed stage ('Stage 3'). Sensitive structures, high rise buildings and

heritage buildings will usually go straight to the third stage (Rankin, 1988). Only Stage 1 and 2 will be discussed in this article.

Building damage up to category 2 can be caused by a variety of environmental phenomena, such as shrinkage, thermal effects on the structure itself, natural movements of the ground due to rising or lowering groundwater, rainfall, drought or tree root suctions. This means that identification of the cause of any category 1 or 2 damage is difficult and could be a combination of causes, whereas category 3 damage is almost certain to be associated with ground movements due to tunnelling if they are occurring at that time. Therefore, the division between category 2 and 3 is important (Burland, 2001). It is also the threshold beyond which repair work starts to become expensive.

Stage 1 assessment

For Stage 1 assessment two criteria are used, the predicted greenfield maximum slope and maximum settlement of the ground surface at the location of each building. If the maximum slope is less than 1/500 and the

maximum settlement is less than 10 mm, then the building has negligible risk of any damage (Rankin, 1988).

It is straightforward, for a given tunnel alignment, to plot contours of surface settlement either side of the tunnel. At this stage of design, settlement estimates are usually based on a Gaussian curve (Peck, 1969), that has the following equation:

$$S = S_{max} \exp\left(\frac{-y^2}{2i^2}\right)$$

Equation 1

where S is the settlement at transverse offset y , S_{max} is the maximum settlement above the tunnel centreline (i.e. at $y = 0$), and i is the trough width, which is the transverse distance from the centreline to the point of inflexion of the Gaussian curve.

Knowing the geology, depth and diameter of the tunnel we can estimate the value of maximum settlement S_{max} and trough width i . The transverse offset y from the tunnel centreline to any settlement contour value S may be found by rearranging Equation 1 to obtain the following expression:

$$y = \sqrt{2i^2 \ln\left(\frac{S_{max}}{S}\right)}$$

Equation 2

Equation 1 can also be differentiated to obtain an equation for slope θ at any offset distance y :

$$\theta = \frac{dS}{dy} = -\frac{y}{i^2} S_{max} \exp\left(\frac{-y^2}{2i^2}\right)$$

Equation 3

Equation 3 can only be solved for y iteratively, which can be achieved using a solver or 'goal seek' function in a spreadsheet.

Equation 2 and Equation 3 can be used to define limits either side of the tunnel on a set of plans of the alignment. All buildings

Category of damage	Normal degree of severity	Description of typical damage (ease of repair is in bold) and typical crack width	Limiting tensile strain ϵ_{lim} (%)
0	Negligible	Hairline cracks < 0.1mm wide.	0-0.05
1	Very slight	Fine cracks that are easily treated during normal redecoration. Damage generally restricted to internal wall finishes. Close inspection may reveal some cracks in external brickwork or masonry. Typical cracks < 1mm.	0.05-0.075
2	Slight	Cracks easily filled. Redecoration probably required. Recurrent cracks can be masked by suitable linings. Cracks may be visible externally and some repointing may be required to ensure weather-tightness. Doors and windows may stick slightly. Typical cracks < 5mm.	0.075-0.15
3	Moderate	The cracks require some opening up and can be patched by a mason. Repointing of external brickwork and possibly a small amount of brickwork to be replaced. Doors and windows sticking. Service pipes may fracture. Weather-tightness often impaired. Typical cracks 5-15mm or several cracks > 3mm.	0.15-0.3
4	Severe	Extensive repair work involving breaking-out and replacing sections of walls, especially over doors and windows. Windows and door frames distorted, floor sloping noticeably. Walls leaning or bulging noticeably, some loss of bearing in beams. Service pipes disrupted. Typical cracks 15-25mm, but also depends on the number of cracks.	> 0.3
5	Very severe	This requires a major repair job involving partial or complete rebuilding. Beams lose bearing, walls lean badly and require shoring. Windows broken with distortion. Danger of instability. Typical cracks > 25mm, but depends on the number of cracks.	> 0.3

Table 1: Classification system for visible damage to building walls (based on Burland et al., 1977; Rankin, 1988; Boscardin & Cording, 1989; Burland, 2001).

that are outside both limits can then be excluded from further analysis. The remaining buildings will be taken forward to Stage 2 assessment.

Stage 2 assessment

In this stage, each building is conservatively assumed to deform to the greenfield settlement profile at the level of the foundations, as shown in Figure 1 for an arbitrary building shown in grey shading. The values of settlement are just an example. Between the points of inflexion the building is bending in a sagging mode, and outside them the building is bending in a hogging mode.

The two parts of the building, of lengths L_{hog} and L_{sag} , are treated separately and these are known as 'partitions'. In the hogging partition

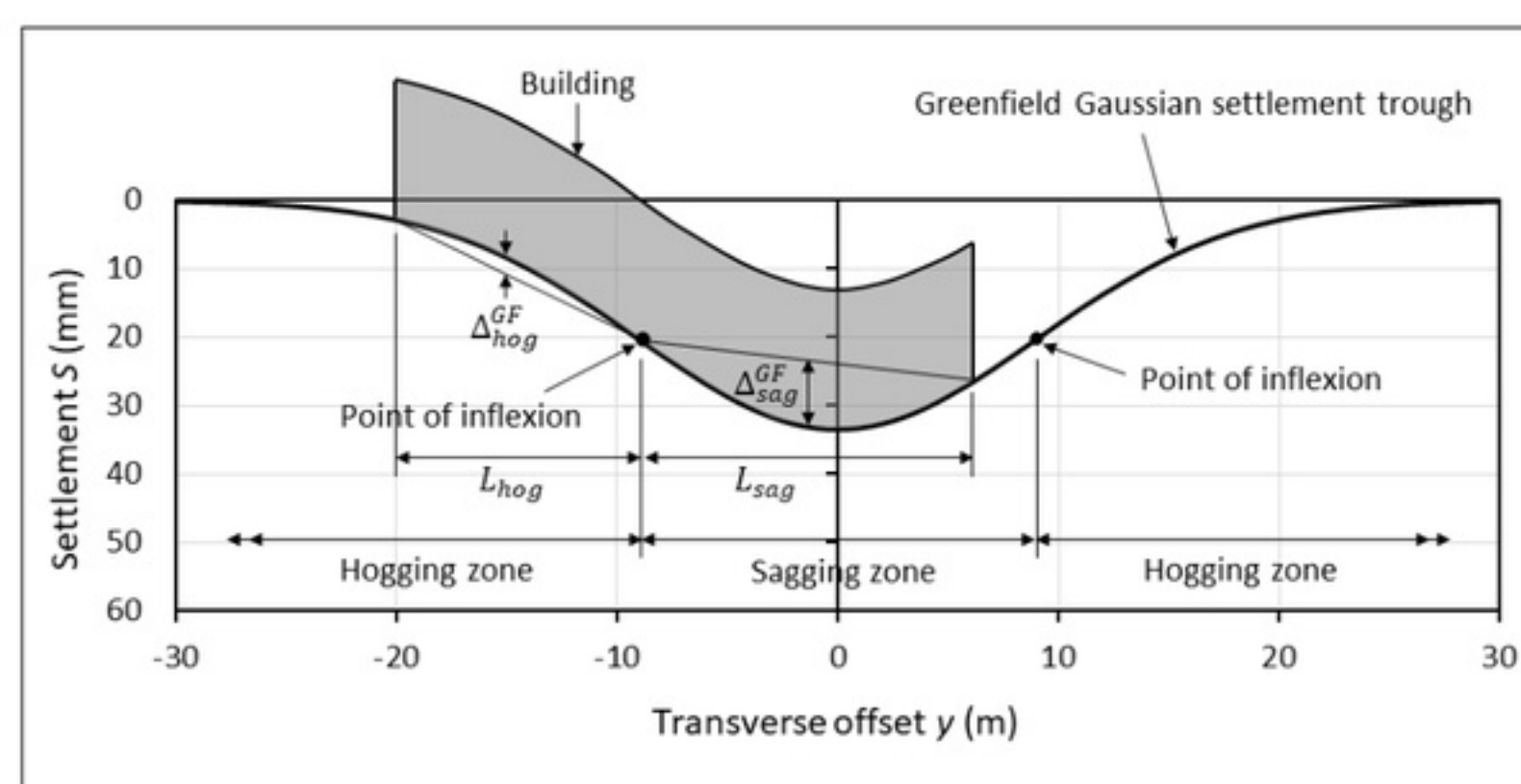


Figure 1: Idealisation of building deformation and definition of deflection ratio (vertical scale much exaggerated).

a straight line is drawn from a point on the settlement trough at the edge of the building to the point of inflexion. The maximum vertical distance between this line and the settlement trough is the deflection Δ_{hog}^{GF} . This deflection divided by the length of the

building in the hogging zone L_{hog} is the hogging deflection ratio. The same procedure is applied to the sagging partition to find the sagging deflection ratio. Note that a long building that spans beyond both points of inflexion may have two hogging zones and therefore

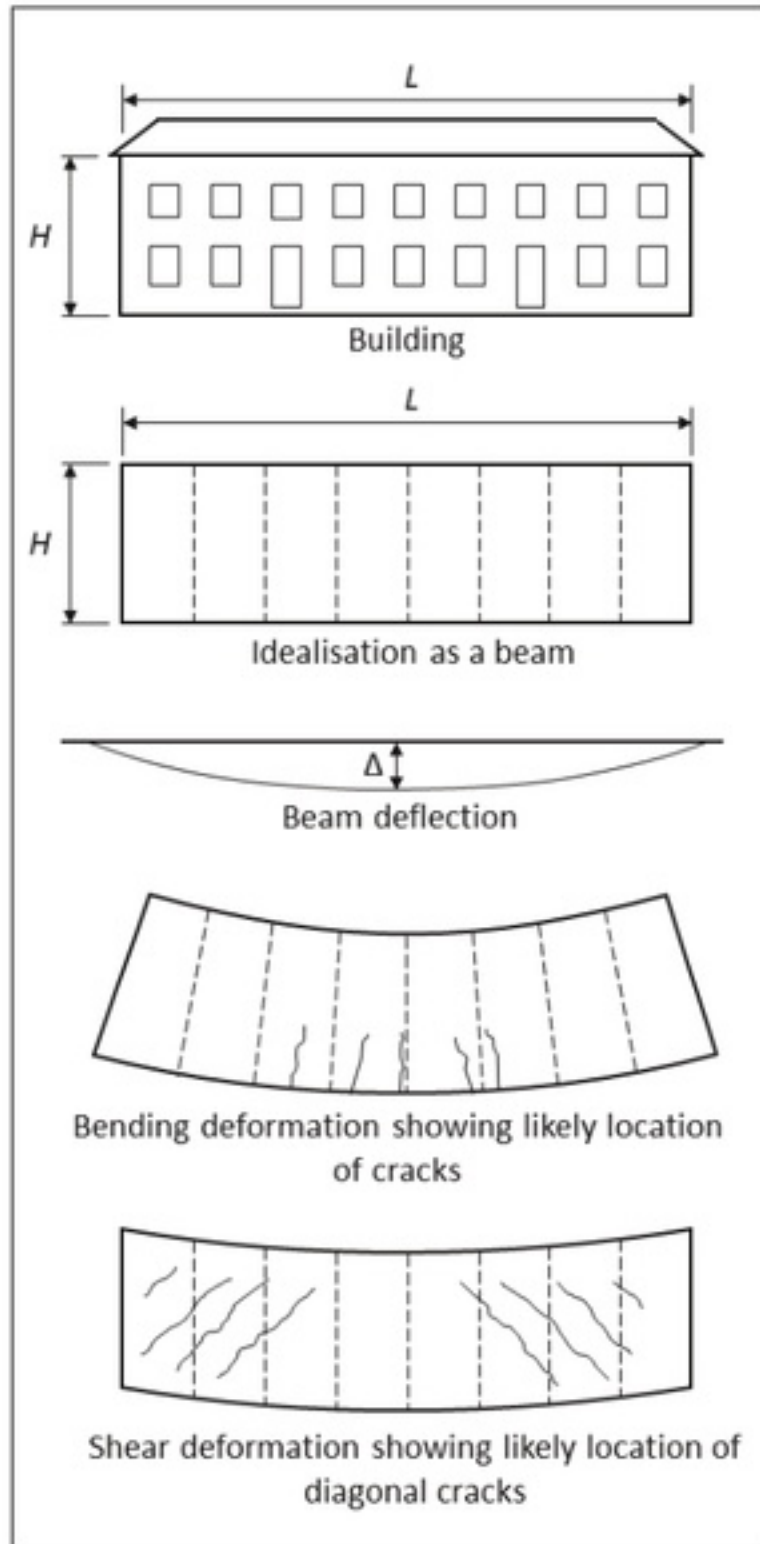


Figure 2: Idealisation of a bearing-wall building façade as a beam (Burland & Wroth, 1974).

two values of hogging deflection ratio will need to be calculated.

The next step is to impose these deflection ratios onto the building. Burland & Wroth (1974) first proposed this should be done by modelling the building as a simple beam under the action of a point load. This will not give the exact deformation mode of the building, but this is only intended to be an approximate method. Figure 2 shows how a bearing-wall building can be idealised as a beam representing the load-bearing façade in bending and shear deformation according to the method of Burland & Wroth (1974), and Figure 3 shows the simply-supported beam with a point load applied at the midspan.

The midspan deflection of a centrally-loaded simply-supported beam including both bending and shear deflection was given by the following equation in Burland & Wroth (1974), which they attributed to Timoshenko (1957):

$$\Delta = \frac{PL^3}{48EI} \left(1 + \frac{18EI}{L^2HG} \right)$$

Equation 4

where Δ is the midspan deflection, P is a centrally-applied line load (c.f. Figure 3), L is the length of the beam and equal to either L_{hog} or L_{sag} , E is the Young's modulus, I is

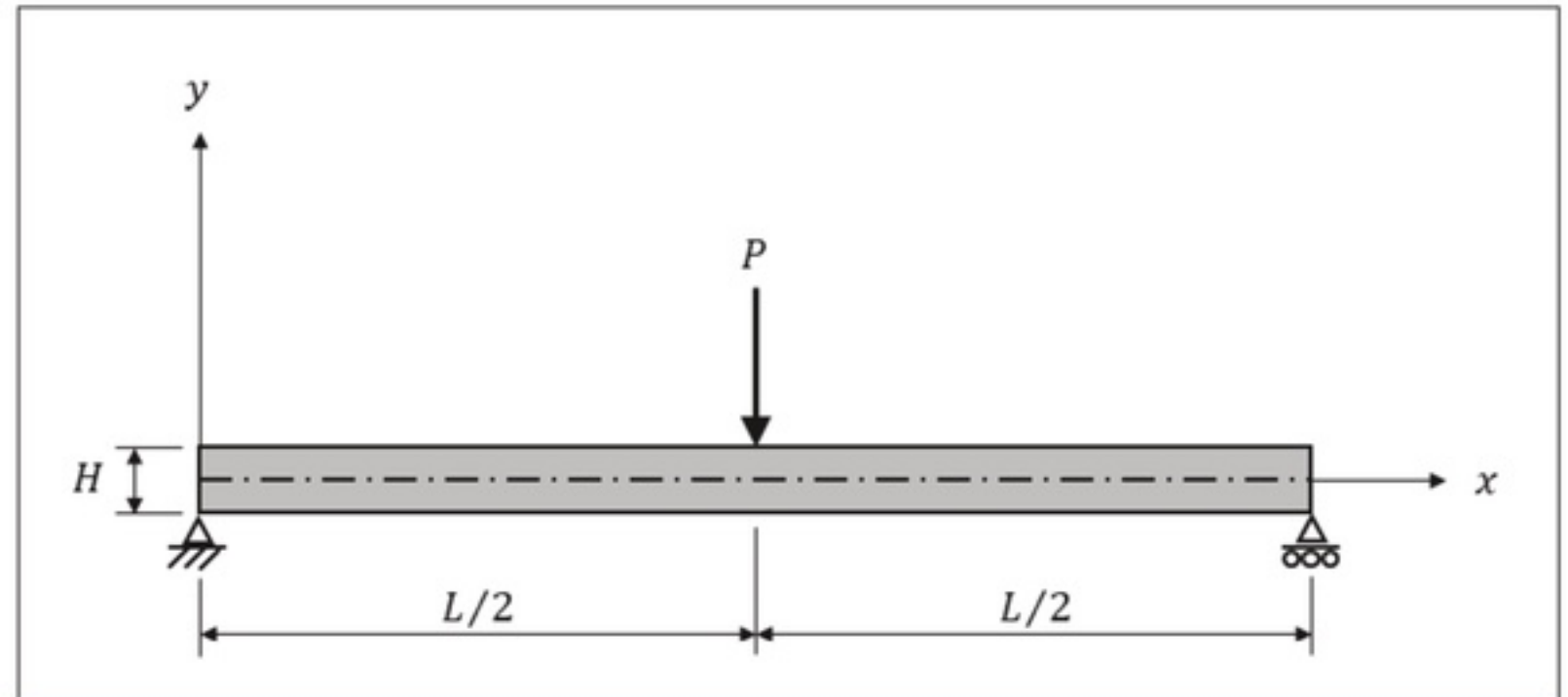


Figure 3: Simply-supported beam with a point load applied at the midspan.

the second moment of area, H is the height of the beam, and G is the shear modulus.

The first term in Equation 4 represents deflection due to bending and the second term represents deflection due to shear. Burland & Wroth (1974) stated that Equation 4 was per unit width of the façade. The original equation from Timoshenko (1940) is shown below, and it can be seen that Burland and Wroth substituted the height H for the area A .

$$\Delta = \frac{PL^3}{48EI} \left(1 + \frac{18EI}{L^2AG} \right)$$

Equation 5

To consider a beam of unit width, not only should the cross-sectional area A in Equation 5 be taken as equal to the height H , but the second moment of area I and the line load P must also be per unit width. Whether a unit width is used for A , I and P , or whether the actual width of the wall is used to calculate A , I and P , will not affect the results, as long as a consistent approach is taken. This becomes important when structures more complicated than a single wall are considered.

Another issue with the deflection equation (Equation 4 or Equation 5) is that it does not calculate shear deflection correctly, because it assumes that simple beam theory (also known as 'Euler-Bernoulli') can also be applied to shear deflection. However, this will not be accurate because the 'shear area', the effective area of a section participating in the shear deformation, is not equal to the cross-section area (e.g. Bhatt, 1999: pp.275-279). This effect is largely to do with warping caused

by the parabolic shear stress distribution, as shown in Figure 4, which means that plane sections do not remain plane.

A review of a large number of studies of shear deflection by Kaneko (1975) found that shear deflection should be significantly lower than predicted using Equation 4 or Equation 5. The impact of this on building damage assessments was first noticed by Netzel (2009) in his PhD thesis, but has not been widely publicised.

The midspan deflection of a simply-supported beam with a centrally-applied point load was given by Gere & Timoshenko (1991: p.694) as:

$$\Delta = \frac{PL^3}{48EI} \left(1 + \frac{12f_sEI}{GAL^2} \right)$$

Equation 6

where f_s is the 'form factor for shear', which is solely a property of the cross-section dimensions of the beam.

The original deflection equation (Equation 4 or Equation 5) contains the assumption that deflection may be calculated by integrating shear strains along the centroid. Therefore, the form factor for shear is effectively assumed to be equal to the ratio of maximum shear stress at the centroid to average shear stress, which is 1.5. Ignoring warping across the width, Gere & Timoshenko (1991) used the unit load method to demonstrate that form factor is exactly 1.2, and Bhatt (1999) used a different method where errors between linear and cubic shear displacements were minimised and also found it to be 1.2. Using more sophisticated

three-dimensional closed form solutions and finite element analysis, Renton (1991), Schramm et al. (1994), Pilkey (2003) and Iyer (2005) have all found that form factor for shear should be approximately 1.2 for rectangular beams when the width of the beam $b < H$.

Since most load-bearing walls may be idealised as rectangular beams with $b < H$, $f_s = 1.2$ can be used and Equation 6 may be rewritten as:

$$\Delta = \frac{PL^3}{48EI} \left(1 + \frac{72EI}{5GAL^2} \right)$$

Equation 7

The shear deflection will be 20% lower in Equation 7 compared to Equation 4 or Equation 5, and as we will see, this means that the maximum tensile strains will be larger. Equation 7 and the equations to follow that are based on it will henceforth be referred to as the 'corrected equations'.

For masonry bearing-wall structures, a masonry façade perpendicular to the tunnel alignment can be considered to act as a single plane strain rectangular section of length L_{hog} or L_{sag} , height H and of unit width. Note that we are ignoring the effect of openings in the façade, such as windows and doors. This is an unconservative assumption because openings will cause stress concentrations where cracks are more likely to initiate and propagate from.

Expressions for maximum bending strain and maximum diagonal strain may be derived to replace P in Equation 7. In this way we can obtain expressions for these maximum strains in terms of deflection ratio.

The midspan bending moment M is given by:

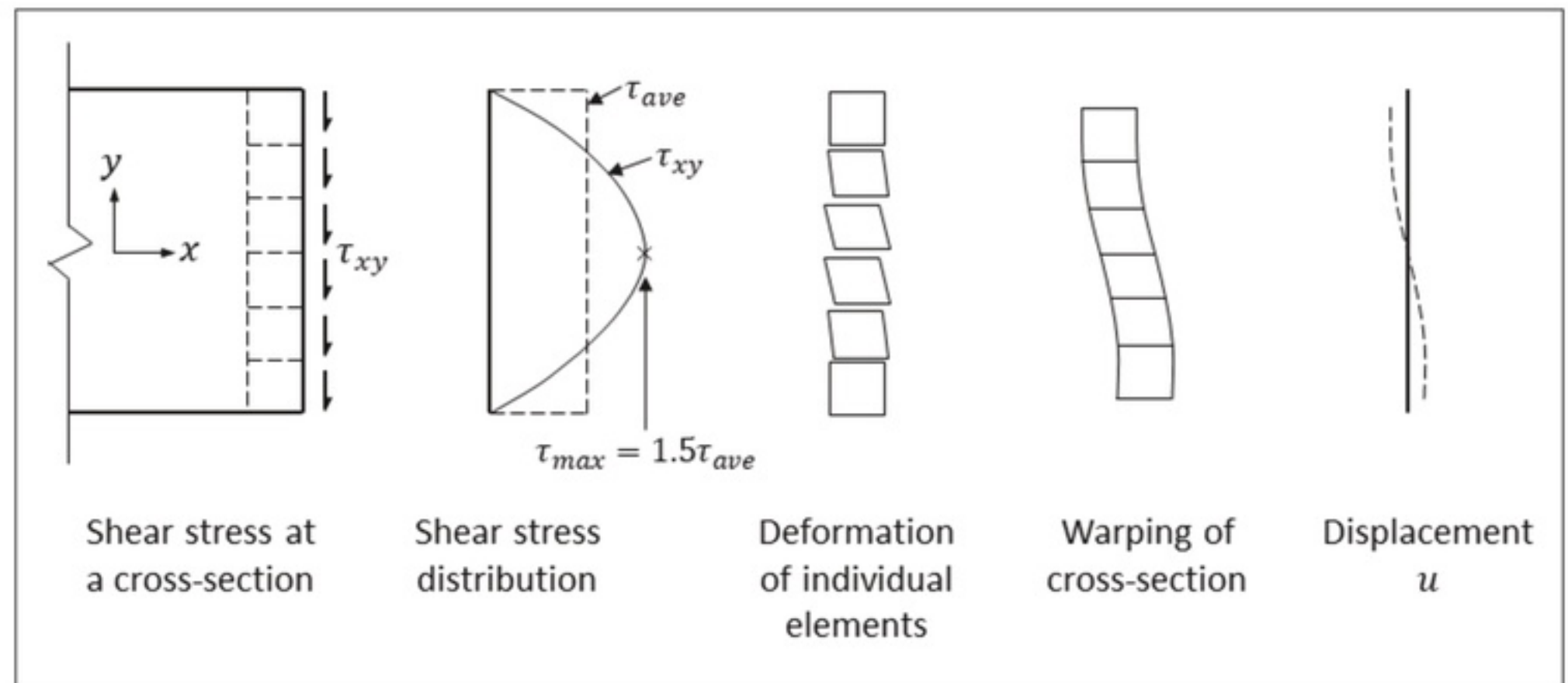
$$M = \frac{PL}{4}$$

Equation 8

The extreme fibre bending stress σ_{bmax} is given by:

$$\sigma_{bmax} = \frac{Md}{I}$$

Equation 9



where d is the vertical distance from the neutral axis to the extreme fibre in tension.

Substituting Equation 8 into Equation 9 gives:

$$\sigma_{bmax} = \frac{PLd}{4I}$$

Equation 10

Therefore, the extreme fibre bending strain ϵ_{bmax} may be given by:

$$\epsilon_{bmax} = \frac{\sigma_{bmax}}{E} = \frac{PLd}{4EI}$$

Equation 11

Rearranging Equation 11 for P gives:

$$P = \frac{4EI}{Ld} \epsilon_{bmax}$$

Equation 12

Substituting Equation 12 into Equation 7 gives:

$$\Delta = \frac{L^2}{12d} \left[1 + \frac{72EI}{5L^2AG} \right] \epsilon_{bmax}$$

Equation 13

We want to calculate ϵ_{bmax} from the deflection ratio Δ/L we have already determined earlier, so rearranging Equation 13 gives:

$$\epsilon_{bmax} = \frac{\Delta/L}{\frac{L}{12d} \left[1 + \frac{72EI}{5L^2AG} \right]}$$

Equation 14

Now to calculate the maximum diagonal tensile strain ϵ_{dmax} we first need an expression relating it to the simply-supported rectangular beam under point load. The shear

strain is related to the shear force by the following expression:

$$\gamma_{xy} = \frac{\alpha V}{AG}$$

Equation 15

where γ_{xy} is the shear strain, α is the ratio of maximum shear stress to average shear stress, which for a rectangular section is 1.5 (c.f. Figure 4), V is the shear force, where $V=P/2$, A is the cross-sectional area, where $A=bH$, and G is the shear modulus.

Substituting for V and α in Equation 15 gives:

$$\gamma_{xy} = \frac{3P}{4AG}$$

Equation 16

Figure 5 defines diagonal extension, which we will call Δ_d . A rectangular element with sides of length dx and dy is deformed into a rhomboid by the action of shear stresses on the sides τ_{xy} and τ_{yx} , where because of equilibrium $\tau_{xy} = \tau_{yx}$. Angles and deformations are assumed to be small and are greatly exaggerated in the figure. The length of the sides of the element do not change as we are considering pure shear.

To get the maximum diagonal tensile strain ϵ_{dmax} we use the following equation:

$$\epsilon_{dmax} = \frac{\Delta_d}{ds} = \frac{\gamma_{xy} dy \cos \theta}{ds}$$

Equation 17

Now $dy/ds = \sin \theta$, therefore:

$$\epsilon_{dmax} = \gamma_{xy} \sin \theta \cos \theta$$

Equation 18

We also know that the direction

Figure 4: Shear warping in a rectangular cross-section beam (based on Bhatt, 1999).

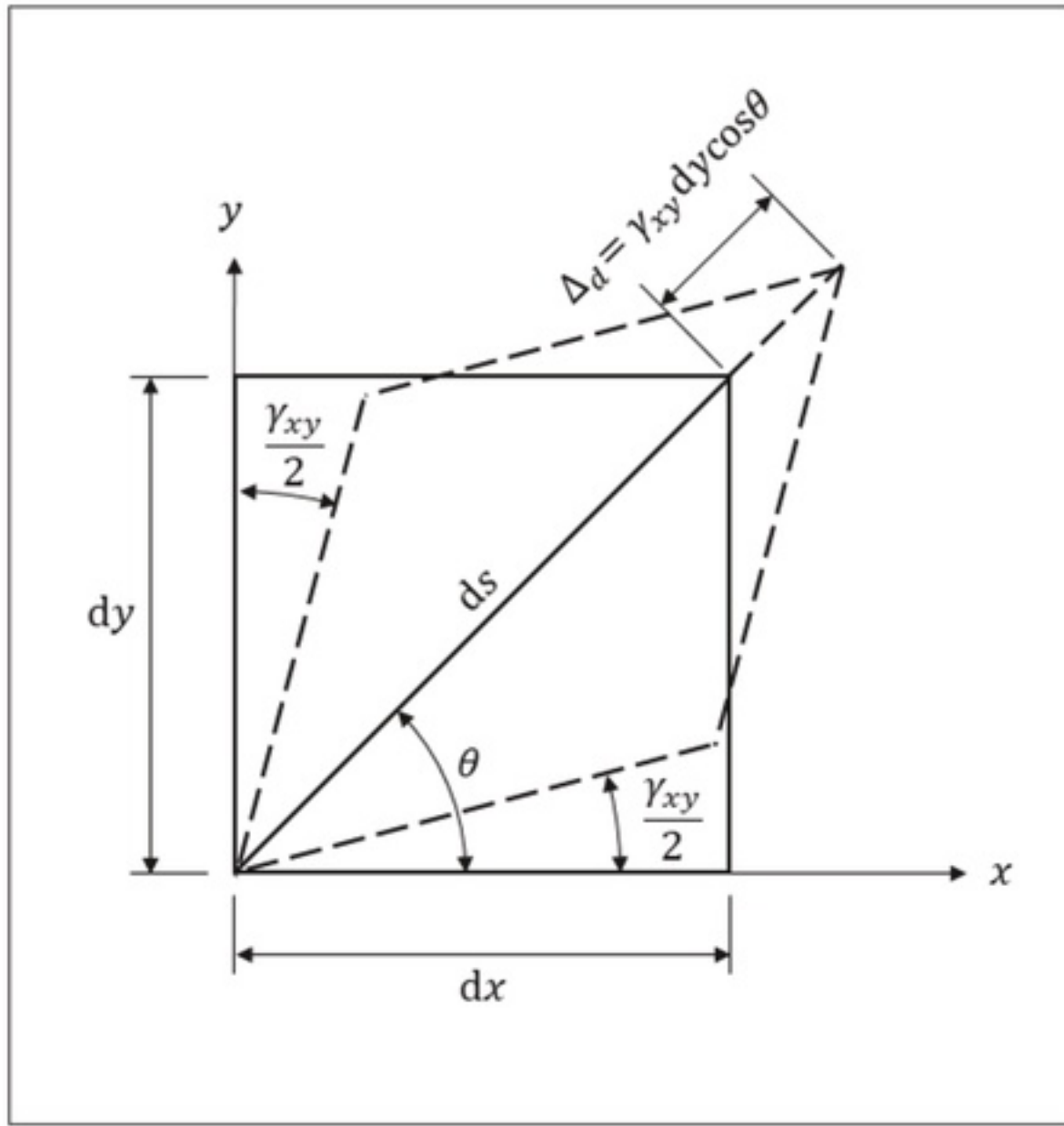


Figure 5: Definition of diagonal extension caused by shear strain.

θ of the maximum diagonal tensile strain is 45° , because shear stresses $\tau_{xy} = \tau_{yx}$. Thus:

$$\epsilon_{dmax} = \frac{\gamma_{xy}}{2}$$

Equation 19

And Equation 16 becomes:

$$\epsilon_{dmax} = \frac{3P}{8AG}$$

Equation 20

Rearranging Equation 20 for P gives:

$$P = \frac{8AG}{3} \epsilon_{dmax}$$

Equation 21

Substituting Equation 21 into Equation 7 gives:

$$\Delta = \frac{AGL^3}{18EI} \left[1 + \frac{72EI}{5L^2AG} \right] \epsilon_{dmax}$$

Equation 22

Similarly to the bending strain we want to calculate the maximum diagonal tensile strain ϵ_{dmax} from the deflection ratio we have already determined earlier, so simplifying and rearranging Equation 22 gives:

$$\epsilon_{dmax} = \frac{\Delta/L}{\left[\frac{AGL^2}{18EI} + \frac{4}{5} \right]}$$

Equation 23

In the sagging zone, the building's neutral axis can be assumed to be at mid-height, i.e. $d=H/2$. Also, assuming plane strain, such that cross-sectional area $A = H$ and the second moment of area is also per unit width, we get the following expression for second moment of area:

$$I_{sag} = \frac{H^3}{12}$$

Equation 24

In the hogging zone, the building's neutral axis is usually conservatively assumed to be at the foundation level, i.e. $d = H$, because the ground-structure interface and the stiffness of the foundations may provide restraint (Burland & Wroth, 1974). Netzel (2009) pointed out that this is physically impossible because the compressive stress becomes infinite, but for materials strong in compression but weak in tension (e.g. masonry, plain concrete or fibre-reinforced concrete at low dosages), the compression zone can become very small and the neutral axis can be very close to the extreme fibre. Therefore, though physically impossible, as a geometric approximation it is reasonable. Using the parallel axis theorem, this gives:

$$I_{hog} = \frac{H^3}{3}$$

Equation 25

So now, from the hogging and sagging greenfield deflection ratios, the maximum bending strain and the maximum diagonal strain in the building in hogging or sagging can be calculated. Remember that the neutral axis position is assumed to be different in each case, which affects the value of second moment of area I and the distance from the neutral axis to the extreme fibre d . The principle of superposition is now employed to add in the effect of horizontal strain to obtain a resultant bending strain and a resultant diagonal strain.

An expression for horizontal strain may be derived from the Gaussian settlement trough equation:

$$\epsilon_h = \left(\frac{-S_{max}}{z_0 - z} \right) \cdot \exp\left(\frac{-y^2}{2i^2} \right) \cdot \left[1 - \frac{y^2}{i^2} \right]$$

Equation 26

For Stage 2 assessment, it is usual practice to use the average horizontal strains under the building's foundation in the hogging and sagging zones, i.e. along L_{hog} and L_{sag} . This was justified by Mair et al. (1996a and 1996b) by arguing that these greenfield horizontal strains are applied to the building, where they are added to tensile strains generated by shear and bending, and the precise location of these strains is unknown. They also argued that the method is effectively empirical and predicts building damage satisfactorily, also bearing in mind that the horizontal strain induced in the building is in many cases considerably less than the greenfield horizontal strain in the ground. Therefore, Equation 26 should be used at, say, 1 m intervals within the hogging or sagging zone to calculate horizontal strains, which are then averaged within each zone to obtain the average values of horizontal strain.

Since the maximum extreme fibre bending strain acts in the same direction as the horizontal axial strain, the resultant extreme fibre tensile strain ϵ_{br} is simply given by:

$$\epsilon_{br} = \epsilon_{bmax} + \epsilon_h$$

Equation 27

The resultant diagonal tensile strain ϵ_{dr} needs to be found using Mohr's circle of strain, because the maximum diagonal tensile strain and the horizontal strain are not in the same direction and the direction and magnitude of the resultant principal strain is therefore unknown.

Two systems of strain are superposed:

1. The horizontal (axial) strain ϵ_h . This is in the beam's x axis direction, therefore we can say that $\epsilon_x = \epsilon_h$. In this system this is the major principal strain, so $\gamma_{xy} = 0$ and using Hooke's Law we also have $\epsilon_y = -\nu\epsilon_h$.
2. The maximum diagonal tensile strain ϵ_{dmax} . This is at 45° to the

beam's x axis. This system is in pure shear, so the major principal strain is ϵ_{dmax} and the minor principal strain is $-\epsilon_{dmax}$. This system can be represented by a shear strain $\gamma_{xy} = 2\epsilon_{dmax}$.

The simplest way of solving this is to use the principal strain equation for plane strain (e.g. Gere & Timoshenko, 1991: p.438), which is:

$$\epsilon_{1,2} = \frac{\epsilon_x + \epsilon_y}{2} \pm \sqrt{\left(\frac{\epsilon_x - \epsilon_y}{2}\right)^2 + \left(\frac{\gamma_{xy}}{2}\right)^2}$$

Equation 28

Since the diagonal strain is pure shear and the horizontal (axial) strain is a principal strain (i.e. with no shear strain), we can say that $\epsilon_x = \epsilon_h$, $\epsilon_y = -\nu\epsilon_h$ and $\gamma_{xy}/2 = \epsilon_{dmax}$, and insert these into Equation 28 such that:

$$\epsilon_{dr} = \frac{\epsilon_h(1-\nu)}{2} + \sqrt{\left(\frac{\epsilon_h(1+\nu)}{2}\right)^2 + (\epsilon_{dmax})^2}$$

Equation 29


The maximum tensile value of either the resultant bending strain ϵ_{br} from Equation 27 or the resultant diagonal strain ϵ_{dr} from Equation 28 will be used to determine the damage category for the building. The maximum diagonal strain ϵ_{dmax} and the maximum bending strain ϵ_{bmax} are not considered in combination with each other because they occur at different locations. The maximum shear strain occurs close to the mid-height of a rectangular beam and is zero at the extreme fibre (c.f. Figure 4), whereas the maximum bending strain occurs at the extreme fibre.

Summary

The main aim of this article was to publicise the shear deflection error first noticed by Netzel (2009). The derivation of the simple beam equations, which has never been published in full, contains hidden assumptions that have been explained in this article, providing clarity to those who use them.

In the next issue, Part 2 will compare the corrected simple beam equations with those of Burland & Wroth (1974), and then will investigate some of the assumptions that need to be made

when using this method, such as the length of the building in the hogging zone, and the effect

of differences in whole-body tilt between hogging and sagging partitions. 

References

- Bhatt, P. (1999). Structures. New Jersey, USA: Prentice Hall.
- Boscardin, M. D. & Cording, E. J. (1989). Building response to excavation-induced settlement. ASCE J. Geot. Engrg 115(1): 1-21.
- Burland, J. B. (2001). Chapter 3: Assessment methods used in design. In Building Response to Tunnelling, Volume 1: Projects and Methods (eds Burland, J. B., Standing, J. R. & Jardine, F. M.), CIRIA Special Publication 200, pp.23-43. London, UK: Thomas Telford Publishing.
- Burland, J. B. & Wroth, C. P. (1974). Settlement of buildings and associated damage – State of the art review. In Conf. on Settlement of Structures, Cambridge, pp.611-654. London, UK: Pentech Press.
- Burland, J. B., Broms, B. B. & de Mello, V. F. B. (1977). Behaviour of foundations and structures. In Proc. 9th Int. Conf. Soil Mechanics and Foundation Engineering, Tokyo, Japan, Session 2, pp. 495-546.
- Crossrail (2008). Crossrail Information Paper D12 – Ground Settlement. London, UK: CLRL.
- Gere, J. M. & Timoshenko, S. P. (1991). Mechanics of Materials, 3rd S. I. Edition. London, UK: Chapman & Hall.
- Iyer, H. (2005). The Effects of Shear Deformation in Rectangular and Wide Flange Sections, MS Thesis, Virginia Polytechnic Institute and State University.
- Kaneko, T. (1975). On Timoshenko's correction for shear in vibrating beams. J. Phys. D: Applied Physics 8: 1927-1936.
- Mair, R. J., Taylor, R. N. & Burland, J. N. (1996a). Prediction of ground movements and assessment of risk of building damage due to bored tunnelling. Proc. Int. Symp. on Geotechnical Aspects of Underground Construction in Soft Ground (eds Mair, R. J. & Taylor, R. N.), London, UK, pp.713-718. Rotterdam, The Netherlands: Balkema.
- Mair, R. J., Taylor, R. N. & Burland, J. N. (1996b). Discussion: Reply to discussion by MP O'Reilly. Proc. Int. Symp. on Geotechnical Aspects of Underground Construction in Soft Ground (eds Mair, R. J. & Taylor, R. N.), London, UK, pp.765-766. Rotterdam, The Netherlands: Balkema.
- Moss, N. A. & Bowers, K. H. (2006). The effect of new tunnel construction under existing metro tunnels. In Proc. 5th Int. Symp. on Geotechnical Aspects of Underground Construction in Soft Ground (eds Bakker, K. J., Bezuijen, A., Broere, W. & Kwast, E. A.), Amsterdam, The Netherlands, 15th-17th June 2005, pp.151-157. London, UK: Taylor & Francis.
- Netzel, H. D. (2009). Building Response due to Ground Movements. PhD thesis, Technische Universiteit Delft. Delft, The Netherlands: Delft University Press.
- Peck, R. B. (1969). Deep excavations and tunnelling in soft ground. In Proc. 7th Int. Conf. Soil Mechanics and Foundation Engrg (7th ICSMFE), Mexico, State-of-the-art report, pp.225-290.
- Pilkey, W. D. (2003). Analysis and design of elastic beams. New York, USA: John Wiley and Sons.
- Rankin, W. J. (1988). Ground movements resulting from urban tunnelling: prediction and effects. Conf. on Engineering Geology of Underground Movements, Nottingham, Geological Society Engineering Geology Special Publication No.5, pp.79-92.
- Renton, J. D. (1991). Generalized beam theory applied to shear stiffness. Int. J. Solids Struct. 27, 1955-1967.
- Schramm, U., Kitis, L., Kang, W., & Pilkey, W. D. (1994). On the shear deformation coefficient in beam theory. Fin. Elem. in Anal. & Design 16, 141-162.
- Timoshenko, S. (1940). Strength of Materials – Part I, 2nd edition. London, UK: D van Nostrand.
- Timoshenko, S. (1957). Strength of materials – Part I, 3rd edition. London, UK: D van Nostrand.

Contact us



Tris Thomas
 Editorial Director
 Tel: + 44 (0) 1892 522 585
 Mobile: + 44 (0) 7812 011 139
 tris@tunnellingjournal.com
 Tunnelling Writer since 1999



Gary Tween
 Managing Director
 Tel: + 44 (0) 1892 522 585
 Mobile: + 44 (0) 7973 205 638
 gary@tunnellingjournal.com
 Tunnelling Media since 2000



Rory Harris
 Chairman
 Mobile: + 1 (859) 321 3164
 rory@tunnellingjournal.com
 Tunnelling Industry since 1987



Kristina Smith
 Contributing Editor
 Mobile: + 44 (0) 7833 230 853
 kristina@tunnellingjournal.com
 Tunnelling Writer since 2010



Daniel Lee-Billinghurst
 Sales Director
 Tel: + 44 (0) 1892 522 585
 Mobile: + 44 (0) 7818 422 712
 daniel@tunnellingjournal.com
 Tunnelling Media since 2001



Mark Piper
 Finance Director
 Mobile: + 44 (0) 7768 554 646
 mark@tunnellingjournal.com
 Tunnelling Industry since 1998



Nicole Robinson
 Contributing Editor
 Mobile: + 44 (0) 7377 792 417
 nicole@tunnellingjournal.com
 Tunnelling writer since 2010



Binda Punj
 Digital Marketing Manager
 Tel: + 44 (0) 1892 710 300
 Mobile: + 44 (0) 7768 275 756
 binda@tunnellingjournal.com
 Tunnelling Media since 2012



Peter Bell
 Director
 Mobile: + 44 (0) 7770 441 867
 peter@tunnellingjournal.com
 Tunnelling Industry since 1984



Amanda Foley
 Contributing Editor
 Mobile: + 44 (0) 7973 158 065
 amanda@tunnellingjournal.com
 Tunnelling Writer since 2000



Michael Hooker
 Art Editor



Steve Caming
 Director
 Mobile: + 1 (603) 662 6263
 stevenaming@gmail.com
 Tunnelling Media since 2001



Now Incorporating World Tunnelling

TGS Media Ltd

The Old Library, Webster House, Dudley Road,
 Tunbridge Wells, Kent TN1 1LE, United Kingdom

Subscription/circulation:

Tel +44 (0) 1892 522585

Email: subs@tunnellingjournal.com

The publishers, authors and printers cannot accept liability for errors or omissions. All rights reserved. No part of this publication may be reproduced in any form without prior permission of the copyright holder and the publisher, application for which should be made to the publisher. TGS Media Ltd. ISSN Tunnelling Journal (Print) ISSN 2044-074X, Tunnelling Journal (Online) ISSN 2044-0758.